Whenever physical signals are measured or generated, the locations of receivers or transducers have to be selected. Most of the time, this appears to be done on an ad hoc basis. For example, when a string of geophones is used in the measurements of seismic data in oil exploration, the receivers are located at equispaced points on an interval. When phased array antennae are constructed, their shapes are determined by certain aperture considerations; round and rectangular shapes are common. When antenna beams are steered electronically, it is done by changing the phases (and sometimes, the amplitudes) of the transducers. Again, these transducers are located in a region of predetermined geometry, and their actual locations within that geometry are chosen via some heuristic procedure.
In all these (and many other) cases, the signals being received or generated are *band-limited.* Optimal representation of such signals has been studied in detail by Slepian et. al. more than 30 years ago, and some of the obtained results were applied by D. Rhodes to the design of antenna patterns; further development of this line of research appears to have been hindered by the absence at the time of necessary numerical tools. We combine these classical results with the recently developed apparatus of Generalized Gaussian Quadratures to construct optimal nodes for the measurement and generation of band-limited signals. In this report, we describe the procedure based on these techniques for the design of such receiver (and transducer) configurations in a variety of environments.

A Procedure for the Design of Apparata for the Measurement and Generation of Band-Limited Signals

V. Rokhlin
Research Report YALEU/DCS/RR-1196
March 29, 2000

The author was supported in part by DARPA/AFOSR under Contract F49620/97/1/0011, in part by ONR under Grant N00014-96-1-0188, an in part by AFOSR under STTR number F49620/98/C/0051
Approved for public release: distribution is unlimited
Keywords: *Band-limited Signals, Antenna Arrays, Beam-forming*

1 Introduction

When measurements are performed, it often happens that the signal to be measured is well approximated by linear combinations of oscillatory exponentials, i.e. functions of the form

$$\sum_{j=1}^{n} \alpha_j \cdot e^{i \cdot \lambda_j \cdot x} \tag{1}$$

in one dimension, of the form

$$\sum_{j=1}^{n} \alpha_j \cdot e^{i \cdot (\lambda_j \cdot x + \mu_j \cdot y)} \tag{2}$$

in two dimensions, and of the form

$$\sum_{j=1}^{n} \alpha_j \cdot e^{i \cdot (\lambda_j \cdot x + \mu_j \cdot y + \nu_j \cdot z)} \tag{3}$$

in three dimensions. In most cases, the signal is band-limited, i.e. there exist such real positive a that all $1 \leq j \leq n$,

$$| \lambda_j | \leq a \tag{4}$$

in one dimension,

$$\lambda_j^2 + \mu_j^2 \leq a^2 \tag{5}$$

in two dimensions, and

$$\lambda_j^2 + \mu_j^2 + \nu^2 \leq a^2, \tag{6}$$

in three dimensions.

As is well-known, most measurements of electromagnetic and acoustic data (especially at reasonably high frequencies) are of this form. Examples of such situations include geophone and hydrophone strings in geophysics, phased array antennae in radar

systems, multiple transceivers in ultrasound imaging, and a number of other applications in astrophysics, medical imaging, non-destructive testing, etc.

In this report, we describe a procedure for determining the optimal distribution of sources and receivers that maximizes accuracy and resolution in measuring band-limited data given a fixed number of receivers. Alternatively, the procedure can be used to determine the optimal distribution of receivers that will minimize their number given specified accuracy and resolution. While the techniques described in this note are fairly general, we describe them in detail in the case of linear antenna arrays; the changes needed to generalize the approach to other cases are summarized in Section 6.

Remark 1.1 One of principal issues in the design of antenna arrays is the treatment (or avoidance) of the so-called supergain (or superdirectivity). Supergain is the condition that occurs when an antenna design is attempted that is prohibited (or nearly prohibited) by the Heisenberg principle; technically, it occurs in the form of very closely spaced elements operating out of phaze, and leads to prohibitive Ohmic losses in transmitting antennae, loss of sensitivity in receiving ones, etc. Since the purpose of this note is to introduce techniques for selecting the locations of elements *for a prescribed antenna pattern*, we avoid the issue of choosing the antenna pattern altogether. Instead, we observe design optimal element distributions for several standard far-field patterns (see Section 5.1), and we observe that the scheme for choosing optimal distributions of elements is virtually independent of the patterns being approximated.

Technically, the approach taken here is to observe that designing an antenna array can be viewed as constructing a quadrature formula for the integration of certain special classes of functions. Using recently developed techniques for the construction of so-called Generalized Gaussian Quadratures, we obtain both nodes and weights that are optimal (in a very strong sense) for the required antenna pattern.

The structure of this note is as follows. In Section 2, we summarize some of the mathematical apparatus to be used: Chebychev Systems, Generalized Gaussian Quadratures,

etc. In Section 3, we recapitulate some of the standard antenna theory, primarily to introduce the necessary notation. In Section 4, element distributions given a specific antenna pattern. In Section 5, we illustrate our approach with several numerical examples, and Section 6 contains a discussion of the generality of the schemes presented.

2 Analytical Preliminaries

In this section, we summarize several known facts about classical Special functions. All of these facts can be found in the literature; detailed references are given in the text.

2.1 Chebyshev systems

Definition 2.1 *A sequence of functions $\phi_1, \ldots, \phi_n$ will be referred to as a* Chebyshev system *on the interval $[a, b]$ if each of them is continuous and the determinant*

$$\begin{vmatrix} \phi_1(x_1) & \cdots & \phi_1(x_n) \\ \vdots & & \vdots \\ \phi_n(x_1) & \cdots & \phi_n(x_n) \end{vmatrix} \tag{7}$$

is nonzero for any sequence of points $x_1, \ldots, x_n$ such that $a \leq x_1 < x_2 \ldots < x_n \leq b$.

An alternate definition of a Chebyshev system is that any linear combination of the functions with nonzero coefficients must have no more than n zeros.

Examples of Chebyshev and extended Chebyshev systems include the following (additional examples can be found in [8]).

Example 2.1 *The powers $1, x, x^2, \ldots, x^n$ form an extended Chebyshev system on the interval $(-\infty, \infty)$.*

Example 2.2 *The exponentials $e^{-\lambda_1 x}, e^{-\lambda_2 x}, \ldots, e^{-\lambda_n x}$ form an extended Chebyshev system for any $\lambda_1, \ldots, \lambda_n > 0$ on the interval $[0, \infty)$.*

Example 2.3 *The functions $1, \cos x, \sin x, \cos 2x, \sin 2x, \ldots, \cos nx, \sin nx$ form a Chebyshev system on the interval $[0, 2\pi]$.*

Example 2.4 *Suppose that $c > 0$ is a real number, w is a positive function $[-1,1] \to \mathbb{R}$ such that $w \in c^1[-1,1]$ and $w(-x) = w(x)$ for all $x \in [-1,1]$, n is a natural number, and the operators $P, Q : L^2[-1,1] \to L^2[-1,1]$ are defined by the formulae*

$$P(\phi)(x) = \int_{-1}^{1} w(t) \cdot e^{i \cdot c \cdot x \cdot t} \cdot \phi(t)\, dt \tag{8}$$

$$Q = P^* \circ P. \tag{9}$$

Suppose further that $\phi_1, \phi_2, \ldots$ are the eigenfunctions of Q, $\lambda_1, \lambda_2, \ldots$ are the corresponding eigenvalues, and $\lambda_1 > \lambda_2 > \lambda_3 \ldots$. Then all eigenfunctions of Q (also known as the right singular vectors of P) can be chosen to be real. Furthermore, the functions $\phi_1, \phi_2, \ldots, \phi_n$ constitute a Chebychev system on the interval $[-1,1]$.

2.2 Generalized Gaussian quadratures

A quadrature rule is an expression of the form

$$\sum_{j=1}^{n} w_j \cdot \phi(x_j), \tag{10}$$

where the points $x_j \in \mathbb{R}$ and coefficients $w_j \in \mathbb{R}$ are referred to as the nodes and weights of the quadrature, respectively. They serve as approximations to integrals of the form

$$\int_a^b \phi(x) \cdot \omega(x) dx \tag{11}$$

with ω is an integrable non-negative function.

Quadratures are typically chosen so that the quadrature (10) is equal to the desired integral (11) for some set of functions, commonly polynomials of some fixed order. Of these, the classical Gaussian quadrature rules consist of n nodes and integrate polynomials of order $2n-1$ exactly. In [13], the notion of a Gaussian quadrature was generalized as follows:

Definition 2.2 *A quadrature formula will be referred to as* Gaussian *with respect to a set of $2n$ functions $\phi_1, \ldots, \phi_{2n} : [a,b] \to \mathbb{R}$ and a weight function $\omega : [a,b] \to \mathbb{R}^+$, if it consists of n weights and nodes, and integrates the functions ϕ_i exactly with the weight function ω for all $i = 1, \ldots, 2n$. The weights and nodes of a Gaussian quadrature will be referred to as Gaussian weights and nodes respectively.*

The following theorem appears to be due to Markov [15, 16]; proofs of it can also be found in [10] and [8] (in a somewhat different form).

Theorem 2.1 *Suppose that the functions $\phi_1, \ldots, \phi_{2n} : [a,b] \to \mathbb{R}$ form a Chebyshev system on $[a,b]$. Suppose in addition that $\omega : [a,b] \to \mathbb{R}$ is a non-negative integrable function $[a,b] \to \mathbb{R}$. Then there exists a unique Gaussian quadrature for the functions $\phi_1, \ldots, \phi_{2n}$ on $[a,b]$ with respect to the weight function ω. The weights of this quadrature are positive.*

Remark 2.1 While the existence of Generalized Gaussian Quadratures was observed more than 100 years ago, the constructions found in [15, 16], [3, 10], [7, 8] do not easily yield numerical algorithms for the design of such quadrature formulae; such algorithms have been constructed recently (see [13, 28, 2]). The version of the procedure found in [2] was used to produce the results presented in the Examples 5.1, 5.2, 5.3 in Section 5.1; the reader is referred to [2] for details.

Applying Theorem 2.1 to the Example 2.4, we obtain the following theorem.

Theorem 2.2 *Suppose that under the conditions of Example 2.4, n is even. Then there exist $n/2$ points $t_1, t_2, \ldots, t_{n/2}$ on the interval $[-1,1]$ and positive real numbers $w_1, w_2, \ldots, w_{n/2}$ such that*

$$\int_{-1}^{1} w(t) \cdot \phi_i(t)\, dt = \sum_{j=1}^{n/2} w_j \cdot \phi_i(t_j), \tag{12}$$

for all $i = 1, 2, \ldots, n$, with $\phi_1, \phi_2, \ldots, \phi_n$ the first n eigenfunctions of the operator Q defined in (9).

Corollary 2.3 *The above theorem provides a tool for the efficient approximate evaluation of integrals of the form (12), as follows. Given a positive real ϵ, we construct the*

Singular Value Decomposition of the operator P defined in (8). Choosing n to be the smallest even integer such that

$$\sum_{j=n+1}^{\infty} \lambda_j^2 < \epsilon^2, \tag{13}$$

we construct an $n/2$-point quadrature that integrates n first right singular functions exactly (effective numerical schemes for the construction of such quadratures can be found in [13, 28, 2]). Now, we observe that due to the triangle inequality combined with the positivity of the obtained weights $w_1, w_2, \ldots, w_{n/2}$,

$$|\sum_{j=1}^{n/2} w_j \cdot e^{i \cdot c \cdot x \cdot t_j} - \int_{-1}^{1} w(x) \cdot e^{i \cdot c \cdot x \cdot t}\, dt| < \epsilon \tag{14}$$

for any $x \in [-1, 1]$.

Remark 2.2 The principal subject of this note is the fact that the pattern of an antenna array is formed by a physical process amounting to a hardware implementation of a quadrature formula for functions of the form (9). Thus, designing a configuration of elements for such an antenna is equivalent to constructing a quadrature formula for functions of the form(9), and can be achieved via the techniques described in [13, 28, 2]).

3 Elements of Antenna Theory

In this section, we summarize certain facts about the theory of linear antenna arrays; all of these facts are well-known, and can be found, for example, in [9].

3.1 Pattern of a linear array

A source distribution σ on the interval $[-1, 1]$ creates the far-field pattern $f : [0, \pi] \to \mathbb{C}$ given by the formula

$$f(\theta) = \int_{-1}^{1} \sigma(u) \cdot e^{i \cdot k \cdot u \cdot cos(\theta)}\, du, \tag{15}$$

where k is the free-space wavenumber, u is the point on the interval $[-1,1]$, and θ is the angle between the point on the horizon where the far field is being evaluated and the x-axis. It is customary to introduce the notation

$$x = cos(\theta), \tag{16}$$

and define the function $F : [-1,1] \to \mathbb{C}$ by the formula

$$F(x) = f(acos(x)). \tag{17}$$

Now, defining the operator $A : L^2[-1,1] \to L^2[-1,1]$ by the formula

$$A(\sigma)(x) = \int_{-1}^{1} \sigma(u) \cdot e^{i \cdot k \cdot u \cdot x} \, du, \tag{18}$$

we observe that

$$F = A(\sigma) = \int_{-1}^{1} \sigma(u) \cdot e^{i \cdot k \cdot u \cdot x} \, du. \tag{19}$$

The function F is usually more convenient to work with than f, and the following obvious lemma is the principal reason for this difference.

Lemma 3.1 *Suppose that $\sigma \in L^2[-1,1]$, the function $F \in L^2[-1,1]$ is defined by (19), α is a real number, and the function $\tilde{\sigma} \in L^2[-1,1]$ is defined by the formula*

$$\tilde{\sigma}(u) = e^{i \cdot \alpha \cdot u} \cdot \sigma(u). \tag{20}$$

Then

$$A(\tilde{\sigma})(x) = A(\sigma)(x - \alpha) \tag{21}$$

for all $x \in (-\infty, \infty)$. In other words, in order to translate the antenna pattern F (viewed as a function of $x = cos(\theta)$) by α, one has to multiply by $e^{i \cdot \alpha \cdot k}$ the source distribution σ generating the pattern F.

Observation 3.1 *While the obvious physical considerations lead to the antenna pattern F defined on the interval $[-1,1]$, the formulae (15), (17) also define naturally the extension of F to the function $\mathbb{R} \to \mathbb{C}$; in a mild abuse of notation, we will be denoting by F both the original mapping $[-1,1] \to \mathbb{C}$ and its extension to the mapping $\mathbb{R} \to \mathbb{C}$. Similarly, we will be denoting by A both the operator $L^2[-1,1] \to L^2[-1,1]$ defined by (18) and its natural extension mapping $L^2[-1,1] \to c^\infty(\mathbb{R})$. The restriction of F on $\mathbb{R}\backslash[-1,1]$ is referred to as the invisible spectrum of the source distribution σ and plays an important role in the antenna theory (this role is discussed briefly in the following subsection). By the same token, the restriction of F on the interval $[-1,1]$ is referred to as the visible spectrum.*

When an antenna array is implemented in hardware, it is (usually) constructed of a finite collection of elements, as opposed to being a continuous source distribution. Mathematically, it is equivalent to replacing the general function σ in (15), (19) with σ defined by the expression

$$\sigma(x) = \sum_{j=1}^{n} \beta_j \cdot \phi_j(u), \tag{22}$$

with $\phi_1, \phi_2, \ldots, \phi_n$ the source distributions generated by individual elements, and the coefficients $\beta_1, \beta_2, \ldots, \beta_n$ the intensities of the elements. As a rule, the elements are localized in space (i.e. the functions $\phi_1, \phi_2, \ldots, \phi_n$ are supported on small subintervals of $[-1,1]$), and very often, all of the elements are identical (i.e. the functions ϕ_j are translates of each other), so that

$$\phi_j(u) = \phi(u - u_j), \tag{23}$$

with ϕ the source distribution of a single element located at the point $u = 0$, and u_j the location of the element number j. Obviously, the far-field pattern of ϕ is given by the formula

$$F_\phi(x) = \int_{-1}^{1} \phi(u) \cdot e^{i \cdot k \cdot u \cdot x} \, du; \tag{24}$$

combining (24) with (22) and (23), we obtain the identity

$$\sigma(x) = \int_{-1}^{1} \phi(u) \cdot e^{i \cdot k \cdot u \cdot x} \, du \cdot \sum_{j=1}^{n} \beta_j \cdot e^{i \cdot k \cdot u_j \cdot x}, \tag{25}$$

known in the antenna theory as the principle of pattern multiplication.

Remark 3.2 The standard form of the principle of multiplication reads: "The field pattern of an array of nonisotropic but similar point sources is the product of the pattern of the individual source and the the pattern of an array of isotropic point sources, having the same locations, relative amplitudes and phases as the nonisotropic point sources" (see [9]). Needless to say, this is a special case of the well-known theorem from the theory of the Fourier Transform, stating that the Fourier transform of the product of two functions is the convolution of the Fourier Transforms of multiplicants.

4 Antenna Patterns and Corresponding Optimal Element Distributions

4.1 Characteristics of an antenna pattern

Depending on the situation, the design of an antenna array attempts to optimize certain characteristics of the resulting far-field pattern, subject to certain constraints on the number, power, etc. of the elements. Since the principal purpose of this note is to describe a technique for the selection of the *locations* of the elements that approximate a user-specified pattern, we could use any reasonable far-field pattern to be approximated. In subsection 4.2, 4.3, we construct optimal element distributions for the so-called sector patterns and cosecant pattern, respectively; a detailed discussion of these (and several other) pattern cans be found, for example in [14].

We will say that the antenna pattern has the ϵ-bandwidth b if

$$\int_{b \le ||x|| \le 1} |F(x)|^2 \, dx = \epsilon^2 \cdot \int_{-1}^{1} |F(x)|^2 \, dx \tag{26}$$

in other words, the proportion of the energy radiated outside the ϵ-beamwidth from the axis of the beam is equal to ϵ. The *supergain* of an antenna is defined (see, for example, [27]), as the ratio

$$\frac{\int_{-\infty}^{+\infty} |F(x)|^2 \, dx}{\int_{-1}^{1} |F(x)|^2 \, dx}. \tag{27}$$

The supergain (sometimes referred to as superdirectivity) measures the ratio of the energy associated with the total spectrum of the antenna to the energy in its visible spectrum; while detailed discussion of supergain and related issues is outside the scope of this note, we will observe that antenna arrays with large degrees of supergain would violate the uncertainty principle, and thus are physically impossible. Attempts to construct supergain antennae result in rapidly (exponentially) growing Ohmic losses, prohibitive accuracy requirements, extremely low bandwidth, etc. Thus, any potentially useful procedure for the design of antenna arrays has to limit the supergain of the resulting patterns.

4.2 Sector patterns

It is often desirable to construct antenna patterns that are as constant as possible within the main beam, and as small as possible outside it; in other words, ideally, the pattern would be defined by the formulae

$$F_b(x) = 1 \quad for \quad |x| \leq b, \tag{28}$$

$$F_b(x) = 0 \quad for \quad |x| > b, \tag{29}$$

with b a real number such that $0 < b \leq k$. Needless to say, the function F_b defined by the formulae (28), (29) is not band-limited, and some approximation has to be used. A standard procedure is to truncate the Fourier Transform of F_b, approximating it by the function $\tilde{F}_b$ defined by the formula

$$\tilde{F}_b(x) = \int_{-1}^{1} \frac{sin(b \cdot t)}{t} \cdot e^{i \cdot k \cdot x \cdot t} \tag{30}$$

(see, for example, [26]). An important special case occurs when $b = k$, with (30) assuming the form

$$\tilde{F}_k(x) = \int_{-1}^{1} \frac{sin(k \cdot t)}{t} \cdot e^{i \cdot k \cdot x \cdot t}; \tag{31}$$

obviously, the latter expression is a band-limited approximation of the δ-function. Another frequently encountered situation is that of $b = k/2$, so that (30) assumes the form

$$\tilde{F}_k(x) = \int_{-1}^{1} \frac{sin(\frac{k}{2} \cdot t)}{t} \cdot e^{i \cdot k \cdot x \cdot t}, \tag{32}$$

which is a band-limited approximation to the beam that is equal to 1 for $-1/2 < x < 1/2$ and to zero elsewhere.

In Section 4.4 below, we demonstrate optimal element configurations that produce approximations to the patterns (31), (32) with $k = 20\pi, 10\pi, 32.4676\pi$.

Remark 4.1 While (30) is by no means the only possible band-limited approximations to to F_b, it is quite satisfactory in most cases, in addition to being simple. Furthermore, the principal purpose of this note is to describe a technique for the selection of *locations* of the nodes, given a pattern to be approximated. Thus, we ignore the issue of the optimal choice of F_b.

4.3 Cosecant patterns

Another standard far-field radiation pattern is the so-called cosecant pattern (see, for example, [19]). Given two real numbers $0 < a < b < 1$, the cosecant pattern $F_{a,b}$ is defined by the formula

$$F_{a,b}(x) = \frac{1}{x} \tag{33}$$

for all $x \in [a, b]$, and

$$F_{a,b}(x) = 0 \tag{34}$$

for all $x \in ([-1,1] \setminus [a,b])$. Again, the function $F_{a,b}$ defined by the formulae (33), (34) is not band-limited, and can not be represented by the expression of the form (24). Before the scheme of this note can be applied to $F_{a,b}$, the latter has to be approximated with a band-limited function; as discussed in Section 4.1 above, if such an approximation is to be useful as an antenna pattern, its supergain factor has to be controlled. Fortunately, a procedure for such an approximation has been in existence for more than 35 years (see, [18]); the algorithm of [18] is a modification of the least-squares approach *permitting the user to limit the supergain factor of the obtained pattern explicitly.* At the time, the utility of the scheme of [18] was limited by the (perceived) difficulty in the numerical evaluation of Prolate Spheroidal Wave functions; given the present state of numerical analysis, this difficulty is non-existent, and it is this author's impression that the insights of [18], [19] deserve more attention than they have been receiving.

4.4 Optimal distributions of elements

In this subsection, we briefly describe an algorithm for the construction of optimal (in the sense defined below) element configurations for the generation of antenna patterns given by (15), of which the patterns (29)-(31) are special cases. As will be seen, the procedure is in fact applicable to the design of element configurations for very general far-field patterns.

We start with observing that (15) expresses the far-field pattern F as an integral over the interval $[-1,1]$ of functions of the form

$$\sigma(u) \cdot e^{i \cdot k \cdot x \cdot u}, \tag{35}$$

with $x = cos(\theta)$ determined by the direction θ in which the far-field is being evaluated. In other words, the problem of finding efficient antenna element distributions is equivalent to that of constructing quadrature formulae for integrals of the form (8), with

$$w(t) = \sigma(t). \tag{36}$$

In the cases when σ is non-negative everywhere on the interval $[-1, 1]$, Theorem 2.2 guarantees the existence of Generalized Gaussian Quadratures, and [13, 28]) provide a satisfactory numerical apparatus for the construction of such quadratures. Obviously, the patterns given by the formula (28) are not generated by non-negative source distributions, except when

$$b \leq \pi. \tag{37}$$

Thus, for these (and many other) patterns, the conditions of Theorem 2.2 are violated, and the existence of Generalized Gaussian Quadratures is not guaranteed. In our numerical experiments, the techniques of [2]) (after some tuning) have always been successful in finding the Gaussian quadratures for integrals of the form (28); some of our results are presented in Section 5 below.

5 Numerical Examples

In this section, we present examples of optimal element distributions generating the patterns of the preceding Section; all of the results presented here have been obtained numerically. Antenna patterns we present are compared to the antenna patterns given by uniform source distributions; configurations of elements approximating these antenna patterns are compared to equispaced distributions of elements generating the same antenna patterns.

5.1 Optimal distributions of elements

In this section, we demonstrate the results of the application of the techniques of Section 4.4 of this note to the types of antenna patterns described in the Sections 4.2, 4.3.

In all cases, we choose the size of an antenna array and a pattern to be reproduced, and use the scheme outlined in Section 4.4 to design a distribution of antenna elements (both the locations and the intensities) located within the chosen array that reproduces the required pattern. For comparison, we also generate optimal (in the least squares sense)

approximations to the desired pattern generated by equispaced elements located within the same array. Since the number of equispaced nodes required to obtain a reasonable approximation to the desired pattern is (in many cases) much greater than the number of optimally chosen nodes, for each example we demonstrate patterns generated by several such configurations. In this manner, the numbers of optimally chosen nodes necessary to obtain reasonable approximations to the desired patterns can be compared to the numbers of equispaced nodes required to obtain similar results.

5.1.1 Sector patterns

Example 5.1 *The first example we consider is of the pattern defined by the formula (32), with* $k = 62.8312$*, so that the size of the array is* 20 *wavelengths.*

In Figure 5, we display an approximation to the pattern obtained with 19 *elements, overlayed with the exact pattern; the locations of the elements are displayed in Figure 5a; the relative error of the obtained approximation is* 5.01%.

Similarly, in Figure 5g, we display the approximation to the pattern obtained with 21 *elements, overlayed with the exact pattern; the relative error of the obtained approximation is* 0.443%*; in Figure 5h, we display the the approximation obtained with* 17 *elements. In the latter case, the relative error of the obtained approximation is* 6.43%*; Figure 5i depicts the* 17*-node distribution producing the approximation illustrated in Figure 5h. Finally, Figure 5j contains a graph of the values of the sources located at the* 17 *nodes depicted in Figure 5i and generating the pattern shown in Figure 5h.*

For comparison, the optimal approximation obtained with 19, 24, 29, 31, *and* 34 *equispaced elements are displayed in Figures 5b, 5c, 5d, 5e, 5f, respectively; these are also overlayed with the exact pattern.*

Example 5.2 *Our second example is identical to the first one, with the exception that* $k = 31.416$*, so that the size of the array is* 10 *wavelengths.*

In Figure 6, we display an approximation to the pattern obtained with 9 *elements, overlayed with the exact pattern; the locations of the elements are displayed in Figure 6a; the relative error of the obtained approximation is* 11.2%.

Similarly, in Figure 6f, we display the approximation to the pattern obtained with 11 *elements, overlayed with the exact pattern; the relative error of the obtained approximation is* 0.600%.

For comparison, the optimal approximation obtained with 9, 14, 16, *and* 18 *equispaced elements are displayed in Figures 6b, 6c, 6d, 5e, respectively; these are also overlayed with the exact pattern.*

Example 5.3 *Our third example is identical to the preceding two, with the exception that* $k = 102$, *so that the size of the array is about* 32.45 *wavelengths.*

In Figure 7a, we display an approximation to the pattern obtained with 23 *optimally distributed elements, overlayed with the exact pattern and with the pattern obtained with* 23 *equispaced elements.*

The relative error of the obtained approximation is 5.4%; *needless to say, the error of the approximation obtained with the equispaced nodes is more than* 70%. *As can be seen from Figure 7c, the actual size of the obtained* 23*-element array is about* 21 *wavelengths; in other words, in order to obtain this precision, the array needs to be about* 2/3 *of the nominal (maximum permitted) length.*

In Figure 7b, we display the approximation to the pattern obtained with 42 *and* 48 *elements, overlayed with the exact pattern.*

It is worth noting that with 33 *optimally distributed elements, the pattern is approximated to the precision* 0.12%; *we do not display the obtained pattern since it is visually indistinguishable from the pattern being approximated.*

Example 5.4 *Our final example is somewhat different from the preceding ones, in that instead of approximating a sector pattern, we approximate a cosecant pattern (see (33), (34) in Subsection 4.3 above).*

In this example, we set

$$a = sin(15^\circ), \tag{38}$$

$$b = sin(75^\circ), \tag{39}$$

and use the procedure of [18] to approximate $F_{a,b}$ with a band-limited function. The band-limit has been more or less arbitrarily set to 110, *resulting in an antenna array about* 35 *wavelengths in size, and the supergain factor of the approximation was set to* 1.1.

In Figure 8a, we display an approximation to the pattern obtained with 53 *optimally distributed elements, overlayed with the exact bandlimited pattern and with the pattern obtained with* 53 *equispaced elements.*

The relative error of the obtained approximation is 1.79%*; the error of the approximation obtained with the equispaced nodes is about* 42%.

In Figure 8b, we display the approximation to the pattern obtained with 47 *optimally distributed elements, overlayed with the exact pattern; the purpose of this final figure is to demonstrate the behavior of the scheme when the number of elements is insufficient (i.e. when the array is underresolved).*

It is worth noting that it takes about 70 *equispaced nodes to obtain the resolution obtained with* 47 *optimally chosen ones.*

The following observations can be made from Figures 5 - 8b, and from the more detailed numerical experiments performed by the author.

1. In order to obtain reasonable precision, the scheme requires about 1 point per wavelength in the antenna array; this is more or less independent from the structure of the beam *as long as the pattern is symmetric about the point* $x = 0$. This fact is observed numerically, even for modest numbers of nodes; for large-scale arrays, this statement (interpreted asymptotically) can be proved rigorously. For certain beam structures, the required number of nodes is even less (see Example 5.3). The reasons for these additional savings are subtle, and have to do with the fact that the continuous source distribution generating the pattern is relatively small on a large part of the antenna array; the algorithm of [2] takes advantage of this fact to reduce the number of nodes. When the beam is not symmetric about $x = 0$, the number of elements required does depend on

the structure of the pattern, and the dependence is fairly complicated. Generally, the improvement for non-symmetric beams is less than that for the symmetric ones.

2. The qualiative behavior of the scheme is similar to that of the Gaussian quadratures in that it displays no convergence at all until a certain minimum number of nodes is achieved; after that, the convergence is very fast. This behavior is not surprising, since the scheme *is* based on a Generalized Gaussian quadrature.

3. For the sector pattern with the sector $[-1/2, 1/2]$, the scheme reduces the required number of nodes by a factor of about 1.5 for small-scale problems, and roughly by a factor of 2 for large-scale ones; again, for large-scale problems, an asymptotic version of this statement can be proven rigorously.

4. For the cosecant pattern with the parameters specified by (38), (39), the number of nodes required is reduced by approximately a factor of 1.4. As the sidelobe level is reduced, the improvement obtained by going from the equispaced discretization to the optimal one increases rapidly.

5. An examination of Figures 5a, 6a shows that while the optimal nodes are by no means uniform, they display no clustering behavior.

6. An examination of Figure 5j shows that the intensities of individual elements do not become large; this is confirmed by the more extensive numerical experiments performed by the author.

7. The combination of the preceding two paragraphs (combined with additional numerical experiments and analysis) provide evidence that configurations of this type should pose no supergain problems.

6 Generalizations

The results described above admit radical generalizations in several directions; several such directions are discussed below,

1. Conformal one-dimensional arrays. The extension of the techniques of this note to one-dimensional arrays located on curves in R^3 is completely straightforward, involving only a modest increase of the CPU time requirements of the procedure. Improvement in the number of nodes required to produce a prescribed pattern is similar to that in the case of a linear array.

2. Planar two-dimensional arrays. A straightforward generalization of the results of Sections 4, 5, is to rectangular planar arrays. Here, a tensor product quadrature can be constructed from the quadratures of Sections 4, 5, possessing all of the desirable properties of the latter. Obviously, the advantage in the number of transducers is squared, so that (for example) replacing 50 nodes in each of the two directions by 23 nodes (see Example 5.3 above) will lead to a factor of $(50/23)^2 \sim 4.7$ savings in the number of elements.

The theory of Section 4 has been extended for disk-shaped arrays, via (*inter alia*) the techniques developed in [23]. The improvement in the number of nodes is comparable to that obtained in the rectangular geometry, and the CPU time requirements do not differ appreciably from those in the case of linear one-dimensional arrays.

The extension of the theory to more general geometries in the plane is in progress. At the present time, our only numerical experiments have been with arrays on triangles; the results are encouraging, but the CPU time requirements of the algorithms are excessive (we have only been able to design triangular arrays about 6 wavelengths in size). We are now in the process of constructing a more efficient numerical procedure for such computations.

3. Conformal two-dimensional arrays. The only environment in which we have a satisfactory theory is when the array is located on a surface of revolution; even in this environment, no experiments have been performed. We have not investigated more general conformal two-dimensional arrays in sufficient detail.

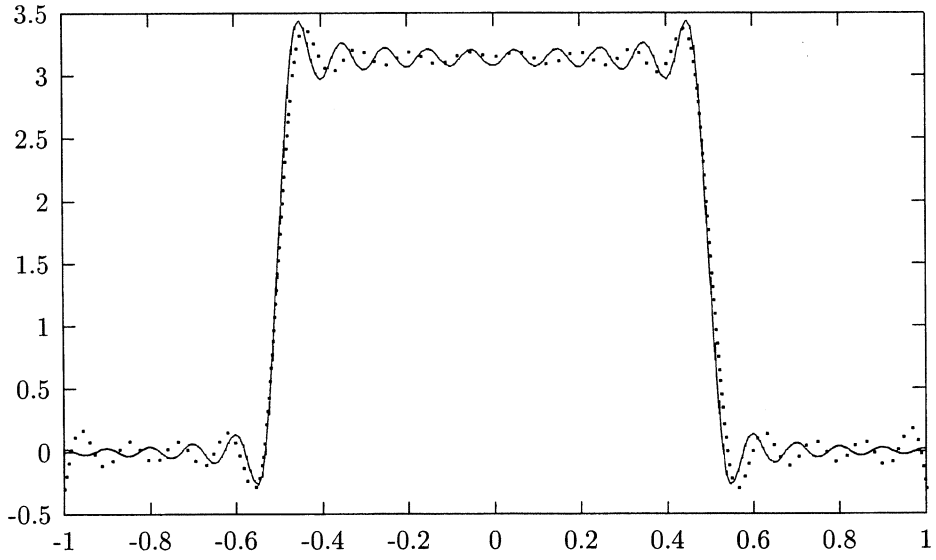

Figure 5: The pattern created by the 19 optimal elements, depicted in Figure 5a as described in Example 5.1

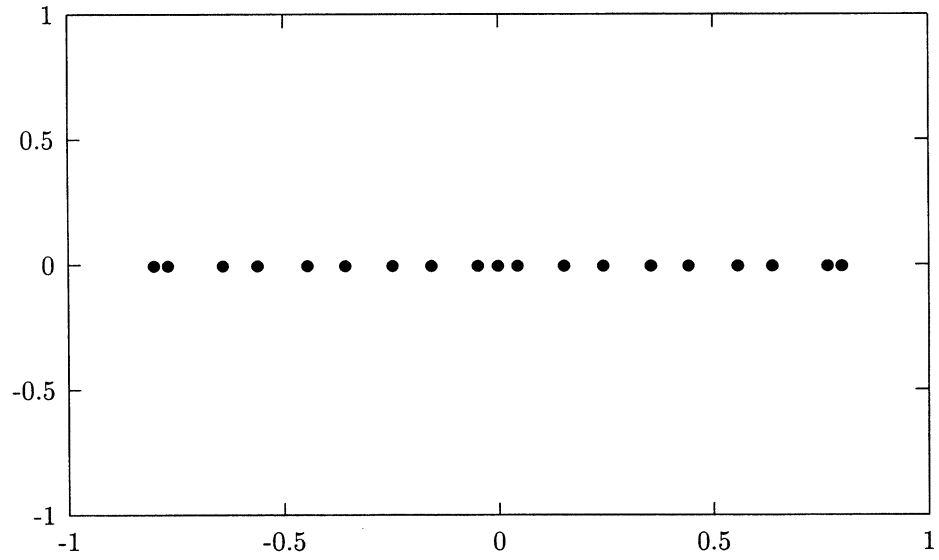

Figure 5a: The distribution of elements creating the pattern depicted in Figure 5, as described in Example 5.1

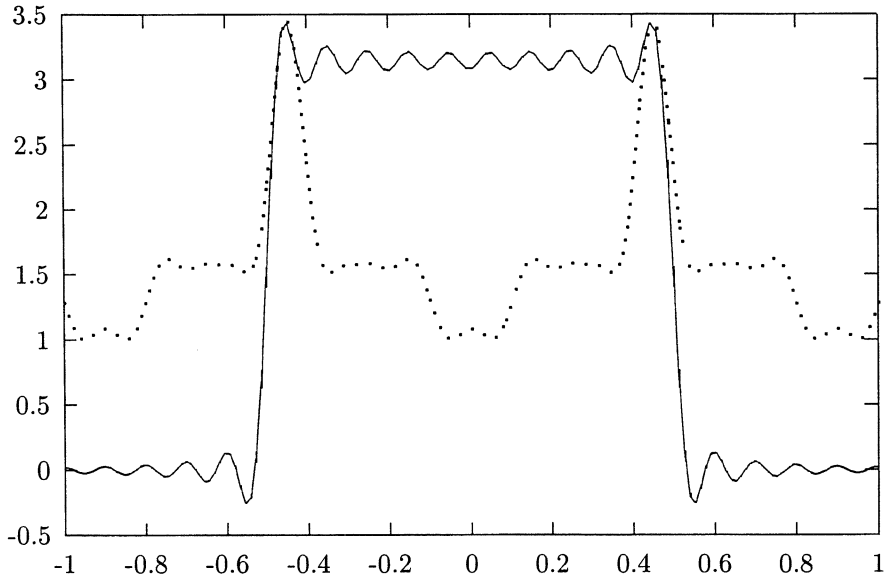

Figure 5b: The optimal approximation to the sector pattern generated by 19 equispaced nodes, as described in Example 5.1

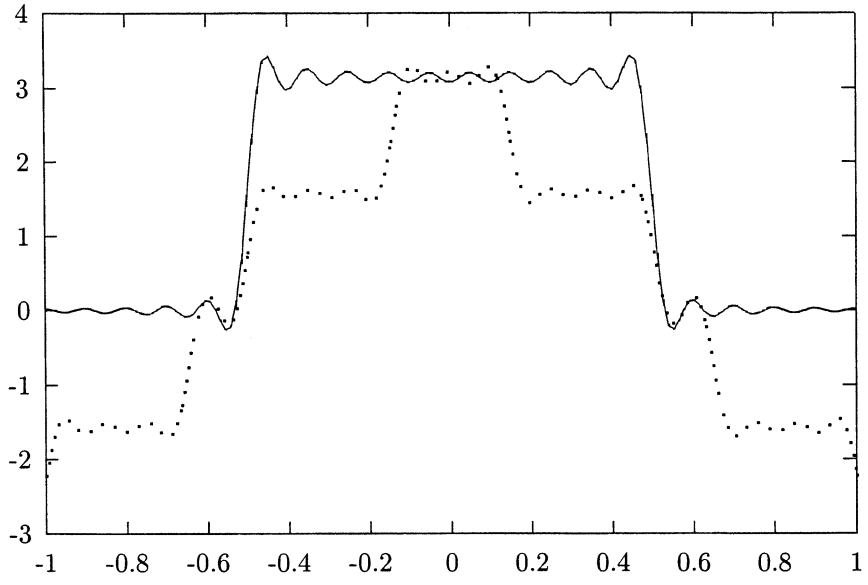

Figure 5c: The optimal approximation to the sector pattern generated by 24 equispaced nodes, as described in Example 5.1

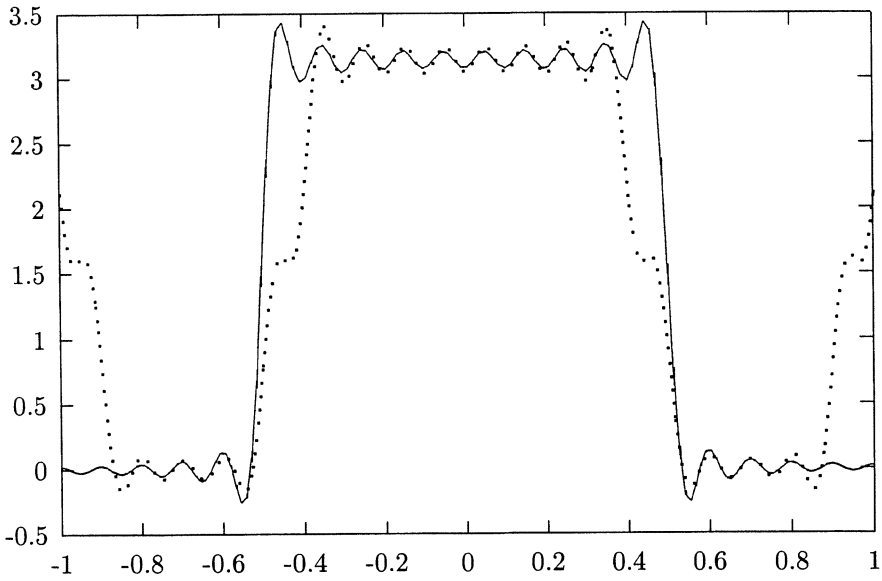

Figure 5d: The optimal approximation to the sector pattern generated by 29 equispaced nodes, as described in Example 5.1

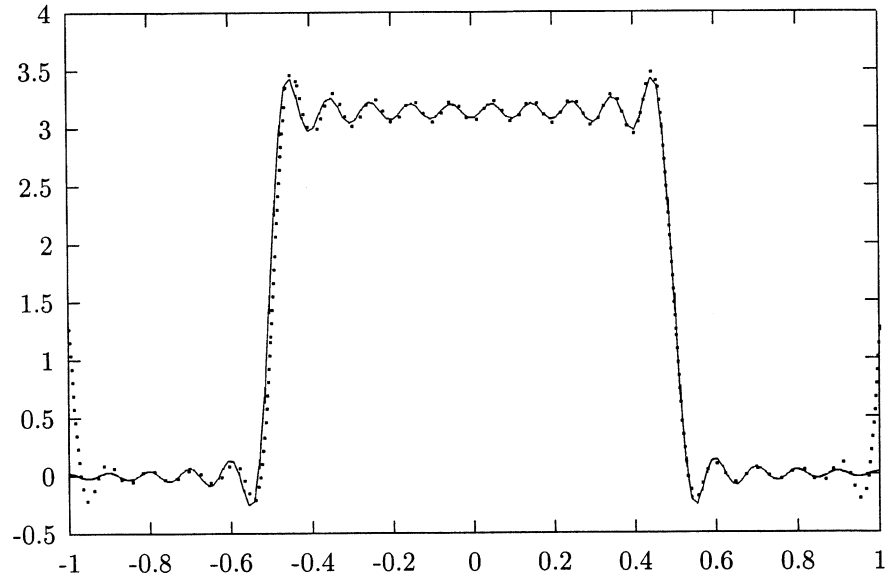

Figure 5e: The optimal approximation to the sector pattern generated by 31 equispaced nodes, as described in Example 5.1

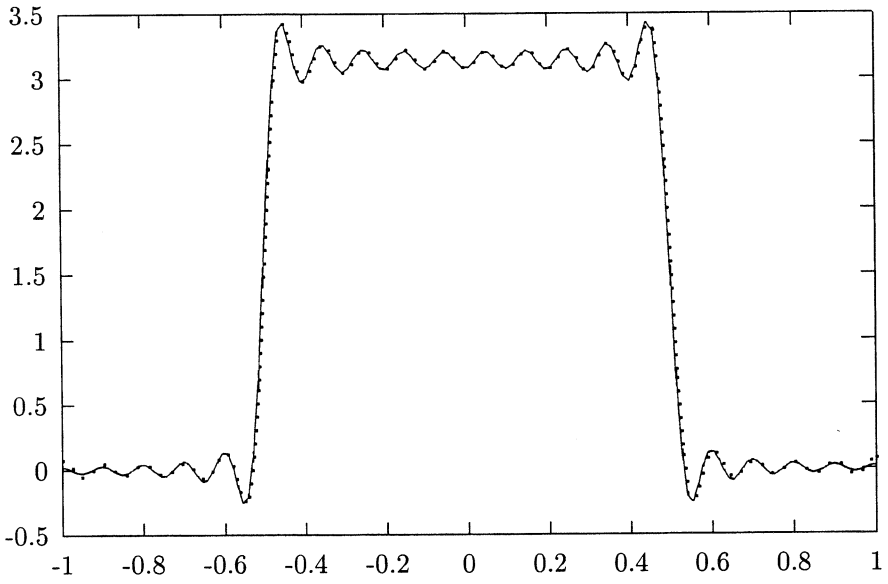

Figure 5f: The optimal approximation to the sector pattern generated by 34 equispaced nodes, as described in Example 5.1

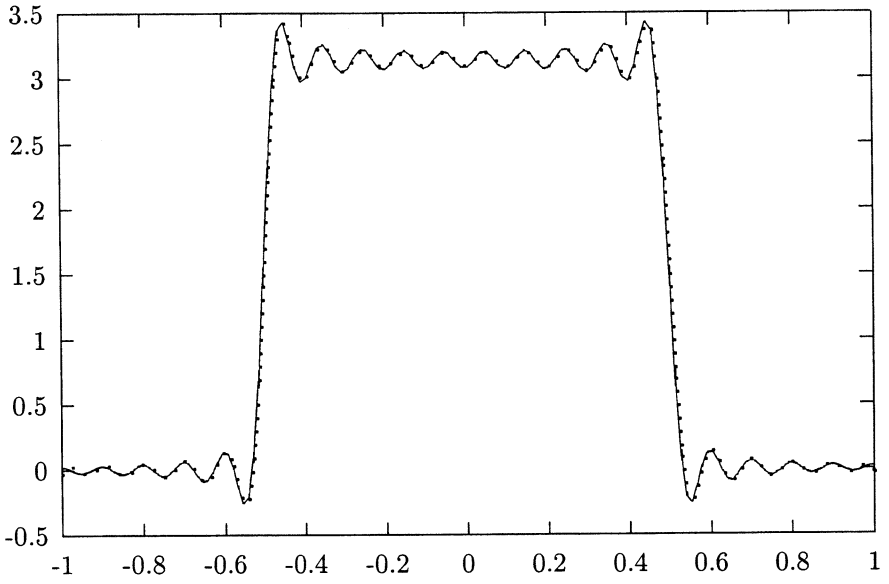

Figure 5g: The optimal approximation to the sector pattern generated by 21 optimal nodes, as described in Example 5.1

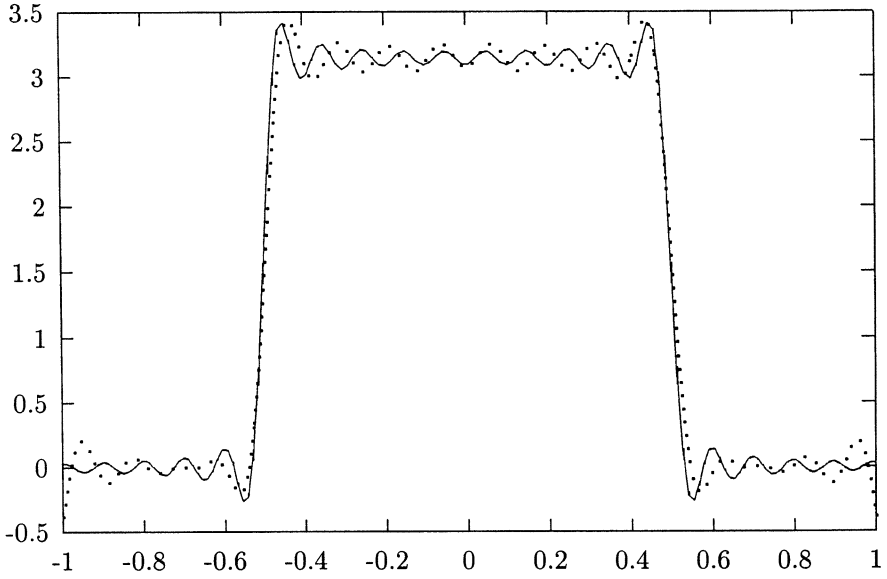

Figure 5h: The optimal approximation to the sector pattern generated by 17 optimal nodes, as described in Example 5.1

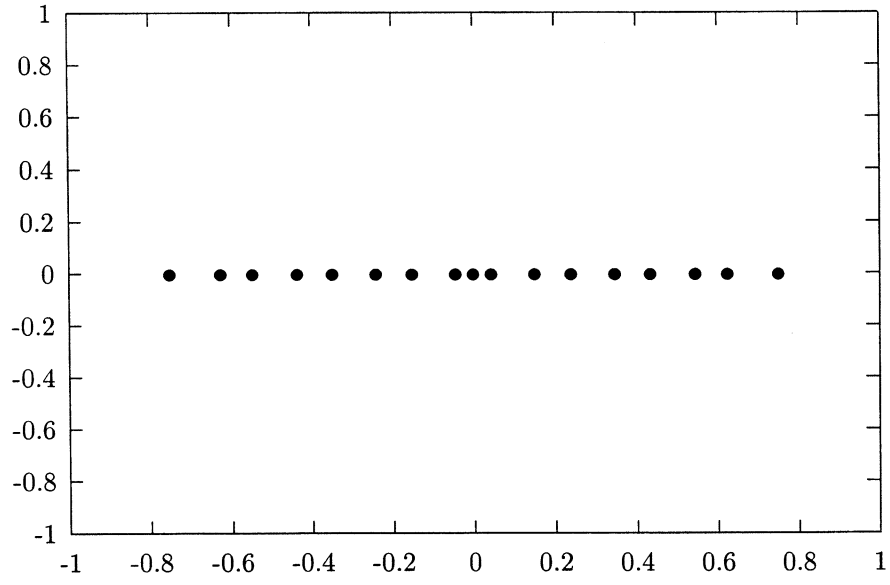

Figure 5i: The distribution of 17 elements creating the pattern depicted in Figure 5h, as described in Example 5.1

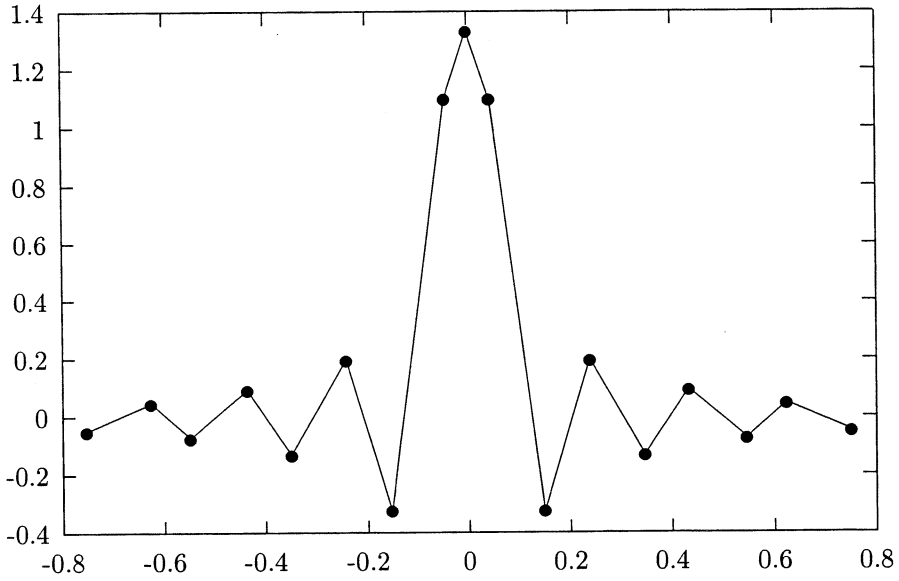

Figure 5j: The values of the sources located at the nodes depicted in Figure 5i and generating the pattern depicted in Figure 5h, as described in Example 5.1

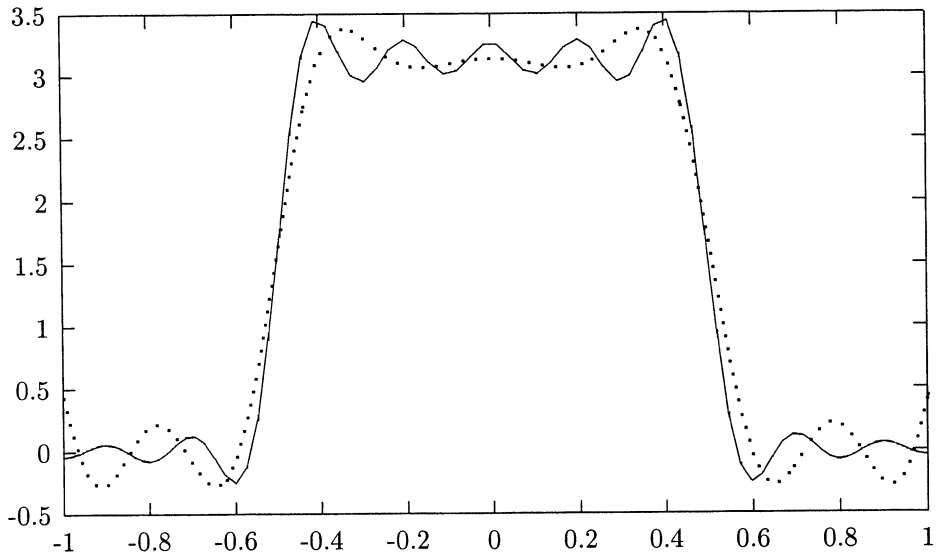

Figure 6: The pattern created by the 9 optimal elements, depicted in Figure 6a as described in Example 5.2

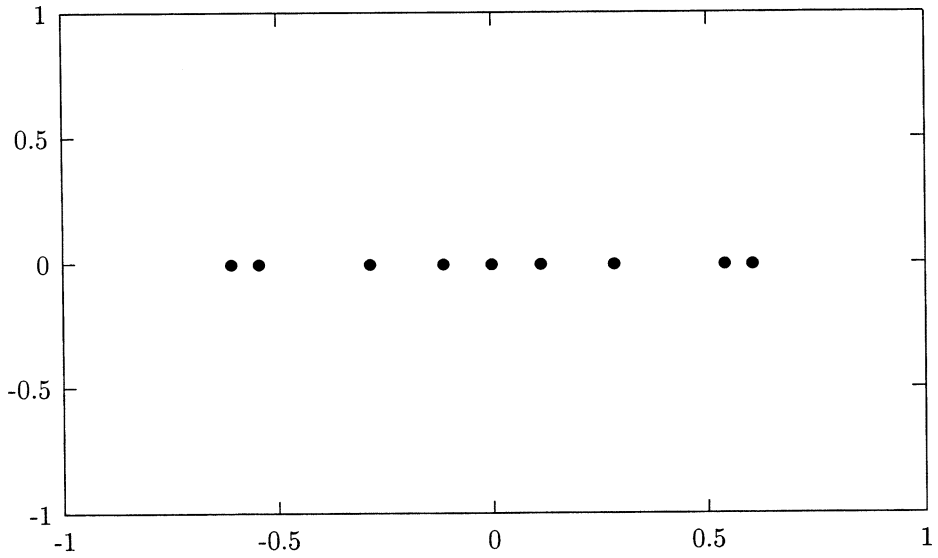

Figure 6a: The distribution of elements creating the pattern depicted in Figure 6, as described in Example 5.2

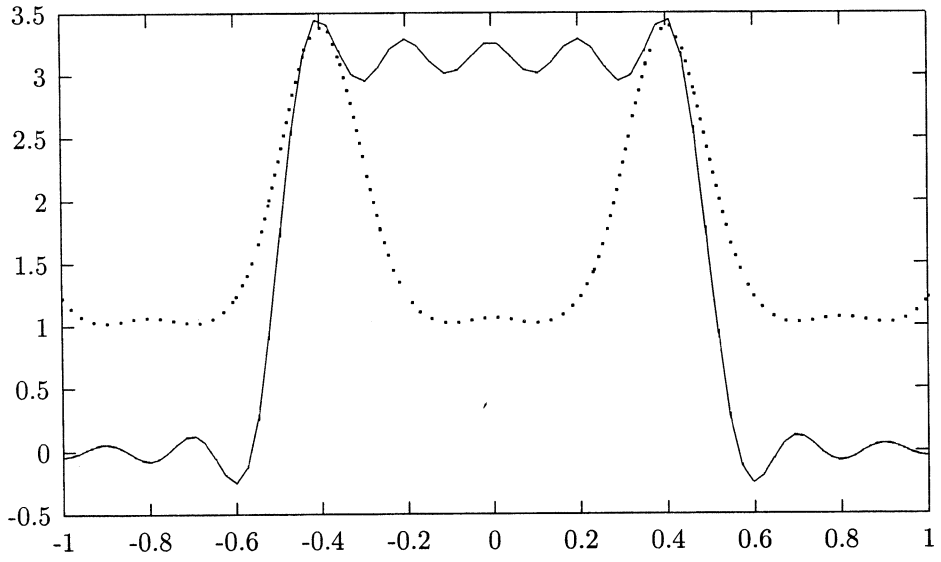

Figure 6b: The optimal approximation to the sector pattern generated by 9 equispaced nodes, as described in Example 5.2

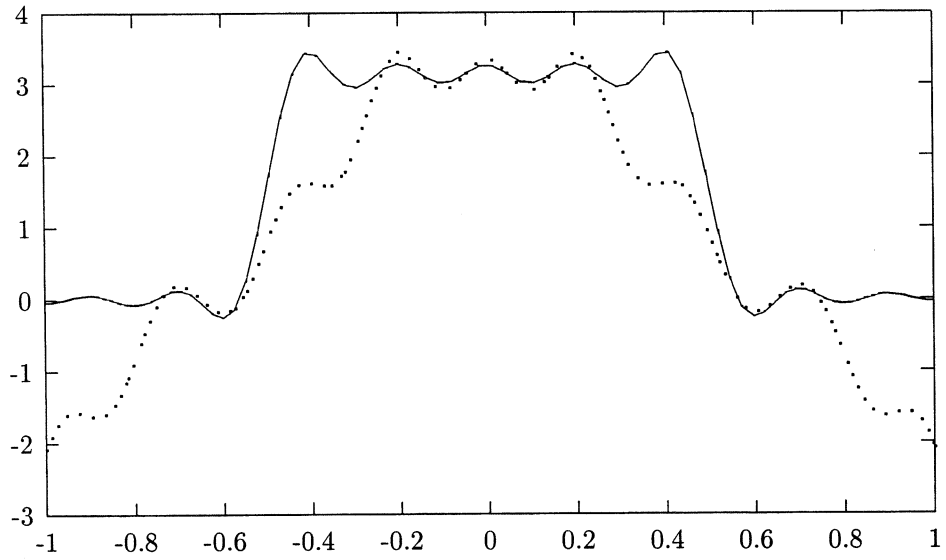

Figure 6c: The optimal approximation to the sector pattern generated by 14 equispaced nodes, as described in Example 5.2

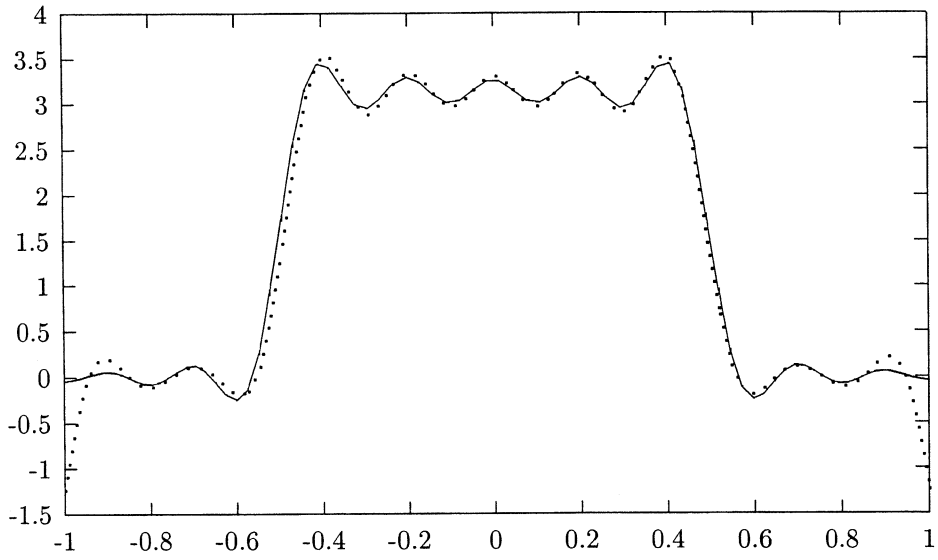

Figure 6d: The optimal approximation to the sector pattern generated by 16 equispaced nodes, as described in Example 5.2

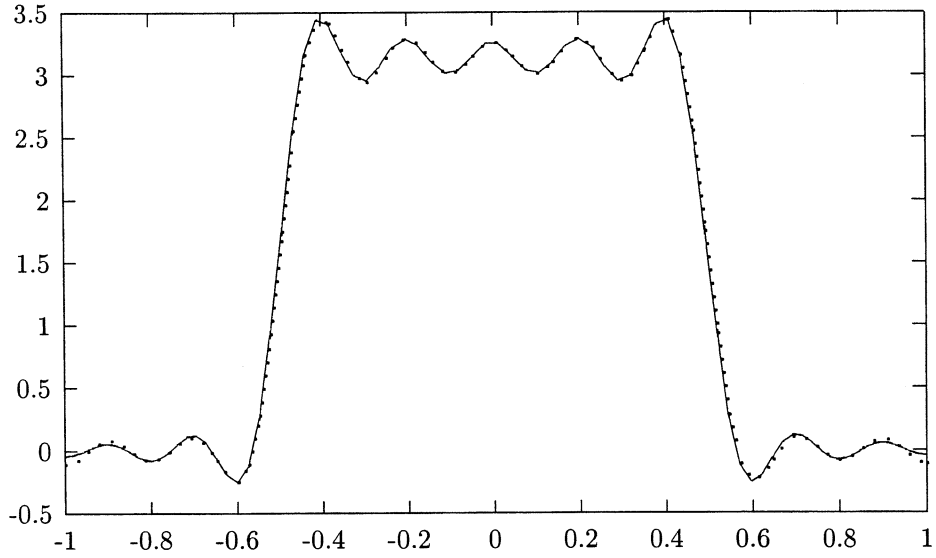

Figure 6e: The optimal approximation to the sector pattern generated by 18 equispaced nodes, as described in Example 5.2

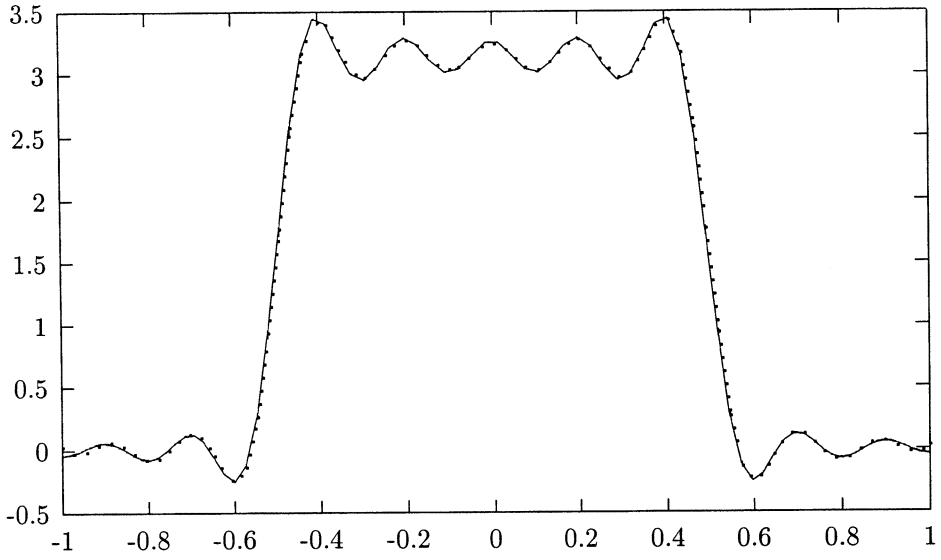

Figure 6f: The pattern created by the 11 optimal elements, in Example 5.2

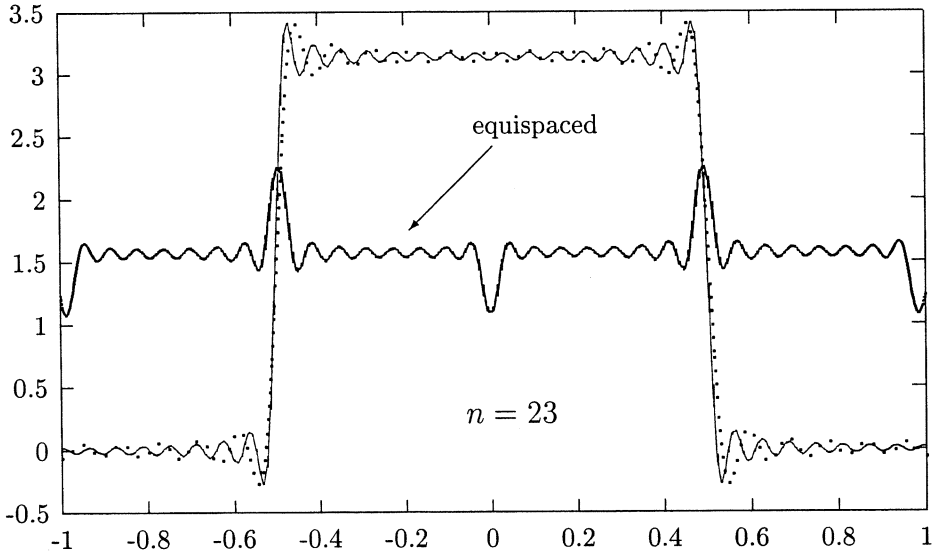

Figure 7a: The approximation to the sector pattern generated by 23 optimal elements, vs. optimal approximation by 23 equispaced nodes, as described in Example 5.3

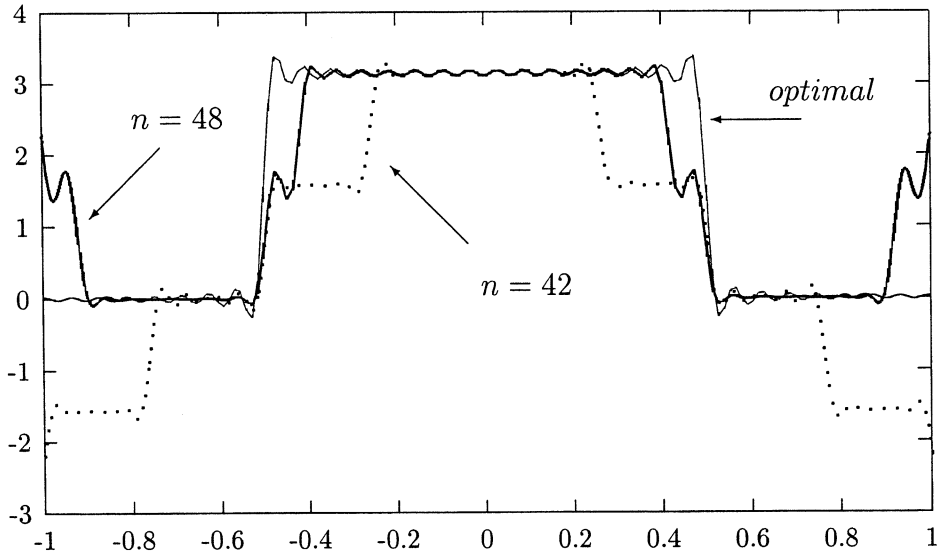

Figure 7b: The optimal approximations to the sector pattern generated by 42 and 48 equispaced nodes, as described in Example 5.3

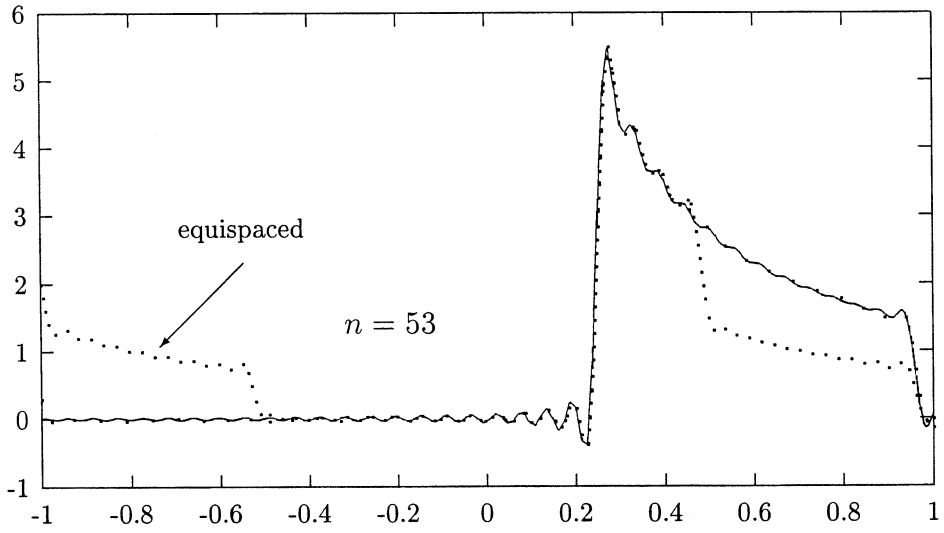

Figure 8a: The approximation to the cosecant pattern generated by 53 optimal elements, vs. optimal approximation by 53 equispaced nodes, as described in Example 5.4

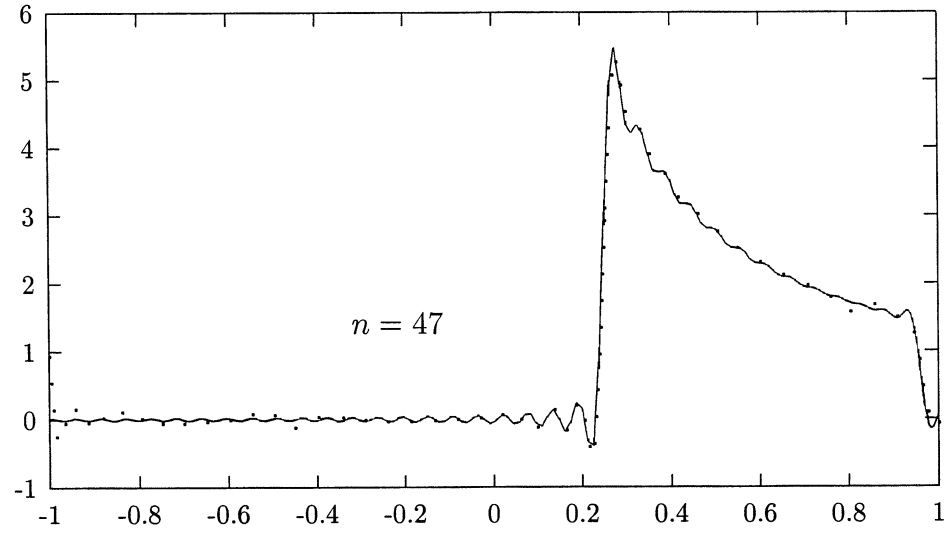

Figure 8a: The approximation to the cosecant pattern generated by 47 optimal elements, as described in Example 5.4

References

[1] M. Abramovitz, I. Stegun, *Handbook of Mathematical Functions*, Applied Math. Series (National Bureau of Standards), Washington, DC, 1964.

[2] H. Cheng, N. Yarvin, V. Rokhlin, *Non-Linear Optimization, Quadrature, and Interpolation*, Yale University Technical Report, YALEU/DCS/RR-1169, 1998, to appear in the SIAM Journal of Non-linear Optimization.

[3] F. GANTMACHER AND M. KREIN, *Oscillation matrices and kernels and small oscillations of mechanical systems*, 2nd ed., Gosudarstv. Izdat. Tehn-Teor. Lit., Moscow, 1950 (Russian).

[4] F. A. Grünbaum, *Toeplitz Matrices Commuting With Tridiagonal Matrices*, J. Linear Alg. and Appl., 40, (1981).

[5] F. A. Grünbaum, *Eigenvectors of a Toeplitz Matrix: Discrete Version of the Prolate Spheroidal Wave Functions*, SIAM J. Alg. Disc. Math., 2(1981).

[6] F. A. Grünbaum, L. Longhi, M. Perlstadt, *Differential Operators Commuting with Finite Convolution Integral Operators: Some Non-Abelian Examples*, SIAM J. Appl. Math. 42(1982).

[7] S. KARLIN, *The Existence of Eigenvalues for Integral Operators*, Trans. Am. Math. Soc. v. 113, pp. 1-17 (1964).

[8] S. KARLIN, AND W. J. STUDDEN, *Tchebycheff Systems with Applications In Analysis And Statistics*, John Wiley (Interscience), New York, 1966.

[9] John D. Kraus, *Antennas*, McGraw-Hill, 1988.

[10] M. G. KREIN, *The Ideas of P. L. Chebyshev and A. A. Markov in the Theory Of Limiting Values Of Integrals*, American Mathematical Society Translations, Ser. 2, Vol. 12, 1959, pp. 1-122.

[11] H.J. Landau, H. Widom, *Eigenvalue Distribution of Time and Frequency Limiting*, Journal of Mathematical Analysis and Applications, 77, 469-481 (1980).

[12] Y.T. Lo, S.W. Lee, editors, *Antenna Handbook, Theory, Applications, and Design*, Van Nostrand Reinhold Company, 1988.

[13] J. MA, V. ROKHLIN, AND S. WANDZURA, *Generalized Gaussian Quadratures For Systems of Arbitrary Functions*, SIAM Journal of Numerical Analysis, v. 33, No. 3, pp. 971-996, 1996.

[14] R.J. Mailloux, *Phased Array Antenna Handbook*, Artech House, 1994.

[15] A. A. MARKOV, *On the limiting values of integrals in connection with interpolation*, Zap. Imp. Akad. Nauk. Fiz.-Mat. Otd. (8) 6 (1898), no.5 (Russian), pp. 146-230 of [16].

[16] A. A. MARKOV, *Selected papers on continued fractions and the theory of functions deviating least from zero*, OGIZ, Moscow-Leningrad, 1948 (Russian).

[17] P.M. Morse, H. Feshbach, *Methods of Theoretical Physics*, McGraw-Hill, New York, 1953.

[18] D. Rhodes, *The optimum line source for the best mean-square approximation to a given radiation pattern*, IEEE Trans. AP, July 1963.

[19] D. Rhodes, *Synthesis of planar antenna sources*, Clarendon Press, Oxford, 1974.

[20] D. Slepian, H.O. Pollak, *Prolate Spheroidal Wave Functions, Fourier Analysis, and Uncertainty - I*, The Bell System Technical Journal, January 1961.

[21] H.J. Landau, H.O. Pollak, *Prolate Spheroidal Wave Functions, Fourier Analysis, and Uncertainty - II*, The Bell System Technical Journal, January 1961.

[22] H.J. Landau, H.O. Pollak, *Prolate Spheroidal Wave Functions, Fourier Analysis, and Uncertainty - III: The Dimension of Space of Essentially Time- and Band-Limited Signals*, The Bell System Technical Journal, July 1962.

[23] D. Slepian, *Prolate Spheroidal Wave Functions, Fourier Analysis, and Uncertainty - IV: Extensions to Many Dimensions, Generalized Prolate Spheroidal Wave Functions*, The Bell System Technical Journal, November 1964.

[24] D. Slepian, *Prolate Spheroidal Wave Functions, Fourier Analysis, and Uncertainty - V: The Discrete Case*, The Bell System Technical Journal, May-June 1978.

[25] D. Slepian, *Some Comments on Fourier Analysis, Uncertainty, and Modeling* SIAM Review, V. 25, No. 3, July 1983.

[26] W.L. Stutzman, G.A. Thiele, *Antenna Theory and Design*, Wiley, 1998.

[27] T.T. Taylor, *Design of Line-Source Antennas for Narrow Beamwidth and Low Side Lobes*, IEEE Trans. on Antennas and Propagation, AP-3, pp. 16-28, 1955.

[28] N. Yarvin and V. Rokhlin, *Generalized Gaussian Quadratures and Singular Value Decompositions of Integral Operators*, SIAM Journal of Scientific Computing, Vol. 20, No. 2, pp. 699-718 (1998).